First-principles Hartree - Fock description of the electronic structure and magnetism of hole and electron states in MnO

1997 J. Phys.: Condens. Matter 9 6591

(http://iopscience.iop.org/0953-8984/9/31/012)

J. Phys.: Condens. Matter **9** (1997) 6591–6606. Printed in the UK PII: S0953-8984(97)83597-7

First-principles Hartree–Fock description of the electronic structure and magnetism of hole and electron states in MnO

W C Mackrodt and E-A Williamson

School of Chemistry, University of St Andrews, St Andrews, Fife KY16 9ST, UK

Received 22 April 1997

Abstract. First-principles periodic Hartree–Fock calculations of the first ionized (hole) state of MnO in both the ferromagnetic and antiferromagnetic AF_{II} spin configurations are reported. Mulliken populations, charge and spin distributions and atom-projected densities of valence band states provide *direct* evidence of O(p) holes in agreement with recent experimental and theoretical studies of NiO. Calculations find the energy of the self-trapped hole to be *lower* than that of the delocalized hole which suggests small-polaron behaviour, in agreement with recent observations. Three different spin arrangements of the hole with respect to the lattice are reported from which the magnetic contributions to the energy are obtained in addition to the lattice relaxation energy associated with an increase in the Mn^{2+}–O^{-} separation. The relaxation energy is close to the reported activation energy for hole conductivity, which further supports small-polaron behaviour of holes in MnO. An excited configuration of the hole state has been determined from broken-symmetry calculations which Mulliken population and *direct* charge and spin distribution analyses suggest is $\sim d^4$. Also reported are similar calculations of the first electron addition state of MnO which indicate that this is essentially a d^6 state. Unlike that of the hole state, the energy of the self-trapped electron is found to be *higher* than that of the delocalized carrier which suggests intermediate- or large-polaron behaviour of the free carrier. However, a localized state is predicted in the presence of an F^{-} substitutional impurity.

1. Introduction

In common with the majority of transition metal chalcogenides, the most interesting (and exploitable) properties of manganese oxides are related to their variable valence. Their electronic structures and defect states, therefore, are of fundamental importance and have been the subject of extensive discussion [1]. In the established tradition of solid-state physics and chemistry the valence states of manganese are designated Mn(I), Mn(II), Mn(III) etc and for practical purposes are most often thought of as Mn^{+}, Mn^{2+}, Mn^{3+} etc. Thus the hole and electron addition states of MnO have been assumed to be Mn^{3+} and Mn^{+} and its defect properties explained largely in these terms. Over the past decade, however, a number of theoretical developments concerning the electronic structure of the 3d oxides suggest that this description of the valence states of manganese might need revision. In 1984 Zaanen, Sawatzky and Allen [2] suggested that the early members of the first-row transition metal oxides are Mott–Hubbard systems with $d \rightarrow d$ gaps, whereas the latter members are $p \rightarrow d$ charge-transfer insulators, with MnO in the intermediate region. Subsequent analysis of the x-ray photoelectron and bremsstrahlung-isochromat spectroscopy of MnO by van Elp *et al* [3] confirmed its position in the Zaanen, Sawatzky and Allen (ZSA)

0953-8984/97/316591+16$19.50

phase diagram, for which there was prior support from self-energy-corrected (SIC) spin-density-functional (LSD) calculations by Svane and Gunnarsson [4], in contrast to earlier band-structure calculations which suggested a d $\rightarrow$ d gap in MnO [5]. Subsequent *ab initio* spin-unrestricted periodic Hartree–Fock (UHF) studies of MnO and NiO [6, 7] found these to be high-spin, p $\rightarrow$ d *charge-transfer* insulators in both the ferromagnetic (FM) and antiferromagnetic (AF) spin arrangements with the majority weight of the valence band edges (VBE) essentially O(p). This suggested that the lowest-energy configurations of the hole states contain strong $d^5\underline{L}$ and $d^8\underline{L}$ components and that the electron addition states are essentially d^6 and d^9 respectively.

More recently, *direct* computational evidence for the O(p) character of holes in Li-doped NiO [8] and the self-trapped hole in NiO [9] has been reported that is based on differences in the UHF charge and spin distributions and densities of unoccupied O(p) states. These results appear to be in good agreement with the theoretical interpretation of the oxygen K-edge x-ray absorption spectra (XAS) by Kuiper *et al* [10] and the nickel 2p XAS edges by van Elp *et al* [11] of $Li_xNi_{1-x}O$ ($x = 0$ to 0.5) and a subsequent cluster calculation analysis of XPS and BIS spectroscopic data in approximately the same doping regime by van Elp *et al* [12].

However, doubts as to the generality of this picture of defect hole states in NiO have been raised by Springhorn and Schmalzried [13] on the basis of conductivity measurements on $(Fe_xNi_{1-x})_{1-\delta}O$, with x in the range 0.05 to 0.1. These authors argued that the dependence of the electrical conductivity on oxygen activity (partial pressure) was incompatible with O(p) holes but consistent with the hopping of Fe(d) holes. Subsequent UHF calculations of the neutral and first ionized state of $Fe_{0.125}Ni_{0.875}O$ [9] have shown that the majority weight of the upper VBE of the neutral system is Fe(t_{2g}) leading to holes in the first ionized state which are essentially of Fe(3d) character in complete agreement with Springhorn and Schmalzried's conclusion [13]. However, this raises a further issue, for given the similarity between the single-particle states in mixed ionic systems of the type $M_xN_{1-x}O$ and the parent oxides MO and NO noted by Towler *et al* [14], it seems likely that a UHF description of FeO would be essentially that of a d $\rightarrow$ d Mott–Hubbard insulator rather than a p $\rightarrow$ d charge-transfer system as suggested by the ZSA classification. It is evident, therefore, that further clarification of the nature of the hole state in MnO would be useful, particularly in view of its intermediate position in the ZSA phase diagram to the 'Mott–Hubbard' side of FeO and the extent to which experimental data have been interpreted on the basis of these systems being essentially Mott–Hubbard systems [1]. Accordingly, this paper reports UHF calculations of the hole state in MnO along the lines previously reported for NiO [9], but including for the first time, we believe, the magnetic structure of the hole and quantitative estimates of the energy of the coupling of the hole to the spin arrangement of the lattice. Such coupling is thought to be an essential feature of high-T_c superconductors [15, 16] and a possible feature that distinguishes cuprates from other first-row transition metal oxides such as manganates and nickelates [17]. It also reports UHF calculations of the electron addition state in MnO.

2. Theoretical procedures

The all-electron *ab initio* LCAO Hartree–Fock method for periodic systems and its computational implementation in the CRYSTAL 95 computer code [18] have been described in detail previously [19]. The calculations reported here use extended Gaussian basis sets and are based on the spin-unrestricted (UHF) procedure of Pople and Nesbet [20] for describing open-shell electronic configurations. The numerical values of the tolerance parameters

involved in the evaluation of the (infinite) Coulomb and exchange series were identical to those used in recent studies [6–9] and chosen, as before, to ensure high numerical accuracy. A detailed account of the effect of these tolerances is discussed elsewhere [21]. The reciprocal-space integration utilized the Monkhorst–Pack sampling [22], with a shrinking factor of 4 (13 k-points in the IBZ and Gilat net), and the SCF convergence criterion based on differences in the total energy of the unit cell of less than 10^{-3} mHartree. The localized crystal orbitals consisted of 24 atomic orbitals for Mn and 14 for O of the type

Mn: 1s(8)2sp(6)3sp(4)4sp(1)5sp(1)3d(4)4d(1)

O: 1s(8)2sp(4)3sp(1)4sp(1)

where the numbers in brackets are the numbers of Gaussian functions used to describe the corresponding shell, e.g. 1s, 2sp and 3d. The exponents and contraction coefficients are those reported previously [7].

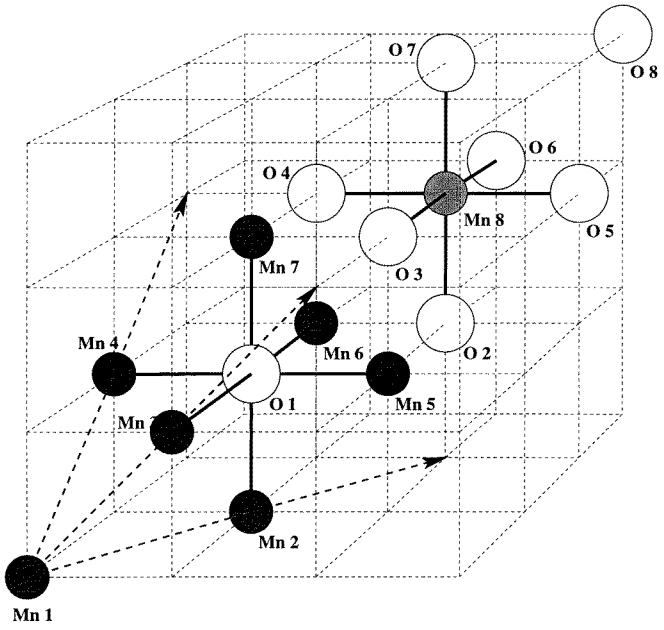

Figure 1. The Mn_8O_8 super-cell structure.

As before [8, 9], we have used a super-cell approach to study both the hole and electron addition states in MnO. For reasons which relate solely to computational resources, not methodology or numerical accuracy, we have been limited to super-cells of composition $Mn_8O_8^{(+)}$, $Mn_8O_8^{(-)}$ and Mn_8O_7F, so the defect concentrations are one per eight formula units. The structure of these super-cells is shown in figure 1 where cations and anions each form two sets of symmetry-inequivalent sublattices, $\{X_1, X_8\}$ and $\{X_2, \ldots, X_7\}$. In the FM arrangement the spins on all of the Mn are parallel, whereas in the AF_{II} arrangement Mn_1, Mn_5, Mn_6 and Mn_7 have opposite spins to those on Mn_2, Mn_3, Mn_4 and Mn_8. Since the hole and electron states are created by electron removal/addition they lead to charged super-cells. To remove the infinite energy that would result from the Coulombic interaction of periodic charged cells, a uniform background charge of opposite sign and equal magnitude is added to the crystal potential, as previously reported [9]. This renormalizes the inter-cell Coulombic

interaction without affecting either the charge distribution or the densities of states, other than by a rigid shift in energy of the single particle spectrum. Since the renormalization energy is a function of the total electron density, the energy difference between states with the same number of electrons (but different spin arrangements or lattice configurations) can be calculated *directly* from total energy differences, whereas that between states with different numbers of electrons cannot. It is for this reason that the band gap cannot be estimated directly from the total energies of hole and electron addition states.

The principal quantities that we have used to examine the nature of the defect states in MnO are *total* energies, which predict *directly* the ground-state charge and spin configuration, Mulliken populations [23], charge- and net spin- ($\uparrow - \downarrow$) density distributions and densities of states (DOS). As emphasized previously [8], while the Mulliken charge is defined in terms of the particular basis set used and is only a guide to the total electron density at a given atomic site, *differences* in the Mulliken charge resulting from structural changes, such as impurity substitution or the addition or removal of electrons, are a reasonable measure of the *change* in the electron density, and it is precisely this change that is of interest here. Furthermore, charge- and spin-density distributions are obtained directly from the wavefunction, so the differences between these distributions for the neutral and first ionized states are, again, a *direct* measure of changes in the charge and spin-density associated with electron removal/addition.

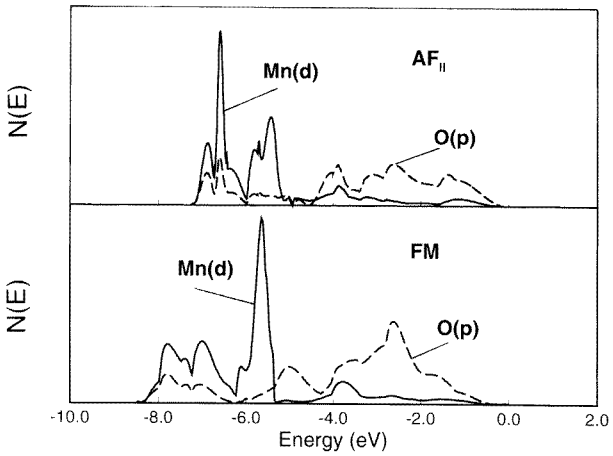

Figure 2. The valence band DOS of FM and AF_{II} MnO.

Table 1. The total Mn Mulliken charge, q_M (e), 3d population, n_{3d}, MnO overlap population, n_{MnO}, and local spin moments, n_s (μ_B), in the FM and AF_{II} states of MnO.

	FM	AF_{II}
q_M	± 1.86	± 1.86
n_{3d}	5.11	5.11
n_{MnO}	-0.02	-0.02
n_s(Mn)	4.92	± 4.92
n_s(O)	0.08	0.0

Table 2. Changes in the total Mulliken charges, δq_M (e), for ls-FM, hs-FM and AF_{II} $Mn_8O_8^{(+)}$, where * denotes the excited configuration, and FM $Mn_8O_8^{(-)}$.

Atom	ls-FM	hs-FM	AF_{II}	AF_{II}^*	FM
Mn_1	+ 0.02	0.0	+ 0.02	+ **0.50**	−0.03
Mn_2	+ 0.01	0.0	+ 0.01	+ 0.02	−0.02
Mn_3	+ 0.01	0.0	+ 0.02	+ 0.02	−0.02
Mn_4	+ 0.02	+ 0.02	+ 0.01	+ 0.02	−0.05
Mn_5	+ 0.02	+ 0.02	+ 0.02	+ 0.02	−**0.76**
Mn_6	+ 0.01	0.0	+ 0.01	+ 0.02	−0.02
Mn_7	+ 0.01	0.0	+ 0.01	+ 0.02	−0.02
Mn_8	+ 0.02	0.0	+ 0.02	+ 0.04	−0.03
O_1	+ **0.76**	+ **0.84**	+ **0.81**	+ 0.02	0.0
O_2	+ 0.02	+ 0.02	+ 0.02	+ 0.01	−0.01
O_3	+ 0.02	+ 0.02	+ 0.01	+ 0.07	−0.01
O_4	+ 0.02	+ 0.02	+ 0.01	+ 0.07	0.0
O_5	+ 0.02	+ 0.02	+ 0.01	+ 0.07	0.0
O_6	+ 0.02	+ 0.02	+ 0.01	+ 0.07	−0.01
O_7	+ 0.02	+ 0.02	+ 0.02	+ 0.01	−0.01
O_8	+ 0.03	+ 0.03	+ 0.02	+ 0.02	0.0

Table 3. Energies, ΔE (eV), of hole state configurations in MnO relative to the infinitesimally distorted low-spin FM state, ls-FM.

Hole state	ΔE
ls-FM	0.0
ls-FM (relaxed)	−0.17
ls-FM (symmetric)	+ 2.33
hs-FM	+ 0.71
hs-FM (relaxed)	+ 0.38
hs-FM (symmetric)	+ 3.16
AF_{II}	+ 0.29
AF_{II} (relaxed)	+ 0.14
AF_{II} (symmetric)	+ 2.80
Excited state AF_{II}	+ 1.00

3. Results

3.1. Neutral MnO

We begin with a brief review of the Hartree–Fock electronic structure and magnetism of MnO [6, 7]. At the lattice constant previously reported, 4.5329 Å [7], the AF_{II} spin arrangement is predicted to be lowest in energy, followed by the ferromagnetic (FM) and AF_I arrangements. The difference in energy between the AF_{II} and FM arrangements is 0.006 eV per MnO. Calculations indicate that the ground states of the three spin arrangements are largely ionic with high-spin d-electron configurations. The total Mulliken charges are ± 1.86 e, the Mn(3d) population is 5.11 and the net spin population of 4.92 is localized entirely on the Mn sites ($t_{2g}^3 e_g^2$) in the AF_{II} arrangement by symmetry, with very little dispersion on O in the ferromagnetic and AF_I states. Full details of the orbital, overlap and spin populations are given in table 1. This description of the $^6A_{1g}$ ground state of MnO is in

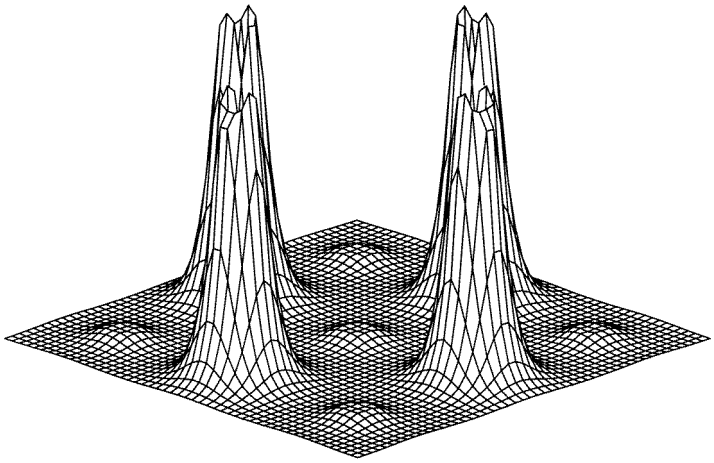

(a)

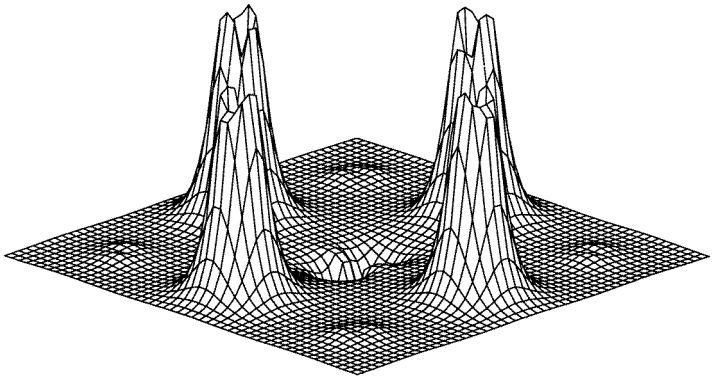

(b)

Figure 3. $(\uparrow - \downarrow)$ spin density in the basal {001} plane of (a) Mn_8O_8, (b) (ls-FM) $Mn_8O_8^{(+)}$, (c) (hs-FM) $Mn_8O_8^{(+)}$ and (d) (AF_{II}) $Mn_8O_8^{(+)}$.

good agreement with that proposed by van Elp *et al* [3] who obtained occupation numbers of 0.85, 0.14 and 0.01 for d^5, $d^6\underline{L}$ and $d^7\underline{L}^2$ respectively from their CI cluster calculation. The valence band is found to be predominantly O(p) at the upper edge in both the FM and AF_{II} spin arrangements, as shown in figure 2, which suggests that the ground configuration of the hole state is $\sim d^5\underline{L}$. In other words, *within a rigid-band approximation*, valence band holes are predicted to be essentially O(p) in character.

3.2. Hole states in MnO

The removal of an electron from a fully symmetric FM lattice in which every site has O_h symmetry leads to a state in which an unpaired electron/hole is delocalized over six oxygen atoms, O_2, ..., O_7, of the $Mn_8O_8^{(+)}$ super-cell *no matter what starting electronic configuration is chosen*. This applies to both high (hs-FM) and low (ls-FM) spin configurations, i.e. where the unpaired spin is parallel or anti-parallel to the ferromagnetic lattice, with the latter $\sim$0.83 eV lower in energy. However, as found previously for NiO

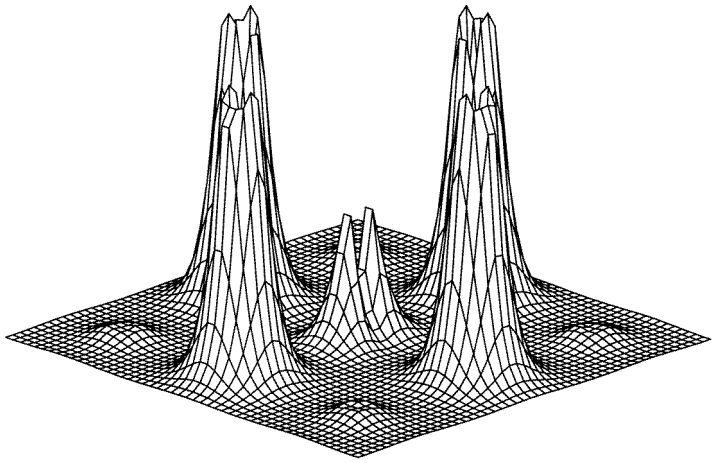

(c)

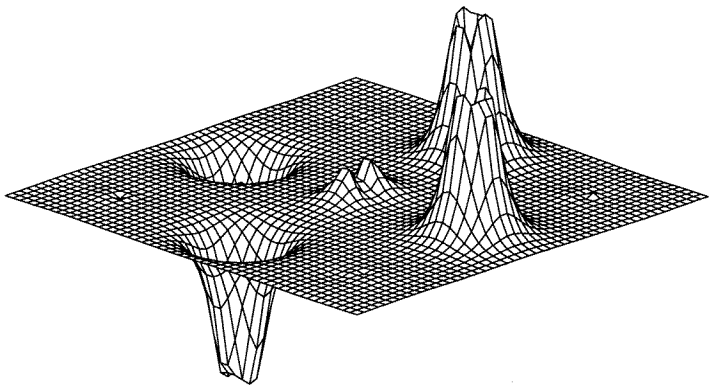

(d)

Figure 3. (Continued)

Table 4. Localization, E_L, Pauli repulsion, E_P (relative to ls-FM), and lattice relaxation, E_R, energies (all in eV) for the hole states in MnO.

State	E_L	E_P	E_R
ls-FM	2.33	0.0	0.17
hs-FM	2.45	0.71	0.33
AF_{II}	2.51	0.29	0.14

[9], the removal of this symmetry constraint allows the electronic configuration to relax to a non-degenerate state of lower energy, in which the unpaired electron/hole is localized on a *single* oxygen site. In particular, a {100} displacement of Mn_5 (or symmetry-equivalent displacements of Mn_2, Mn_3 etc) reduces the local symmetry of O_1 from O_h to C_{4v} which splits the degeneracy of the O_1 p manifold into σ- and π-states with respect to Mn_5. For both spin configurations this leads to localization of the unpaired electron/hole in a p_σ orbital at O_1, exactly as in Ni_7O_8 [9]. For infinitesimal (0.001 Å) displacements of Mn_5

Table 5. Energies, ΔE and $\Delta E'$ (eV), of the electron addition state $Mn_8O_8^{(-)}$ and Mn_8O_7F relative to the infinitesimally distorted FM state.

Electron state	ΔE	$\Delta E'$
FM	0.0	0.0
FM (relaxed)	−0.08	−0.07
FM (symmetric)	−0.24	+ 1.32

the self-trapping energies (relative to the delocalized states) are 2.33 eV and 2.45 eV for ls-FM and hs-FM respectively, with further relaxation energies of 0.17 eV and 0.33 eV at the minimum energy displacements of 0.16 Å and 0.20 Å *away* from the localized hole. The corresponding *changes* in the Mulliken populations are listed in table 2. These suggest that, as found previously for NiO [9], ∼80% of the hole is localized at a *single* oxygen atom, O_1, in both spin configurations, with no more than 3% on any other single site. The local moments at O_1 are $-0.83\ \mu_B$ and $1.02\ \mu_B$ for ls-FM and hs-FM respectively, which testifies further to the localized nature of the hole.

The removal of an electron from a fully symmetric AF_{II} lattice leads to a delocalized hole state, as before, but in this case there is only one spin configuration. However, there are two distinct ways in which the symmetry of the lattice can be broken corresponding to displacements of Mn_4 or Mn_5 which have opposite spins. For displacements in which the unpaired (defect) spin is parallel to the spin of the displaced Mn, the hole localizes in a p_σ orbital at O_1, exactly as before, in a state which is 0.29 eV *higher* than the low-spin FM state. The self-trapping energy is 2.51 eV and the lattice relaxation energy is 0.15 eV at a displacement of 0.14 Å away from the hole. Once again, a Mulliken analysis suggests that ∼79% of the hole is localized at O_1.

It is clear that more extensive relaxations of both the FM and AF_{II} lattice involving neighbouring Mn atoms will increase the trapping energy and that other, more complicated local distortions will also lead to self-trapping of the unpaired electron/hole, but these have not been investigated in detail in the present study. Full details of the energies of the hole states and the corresponding Mulliken populations are given in tables 2–5. In table 4 the localization energy, E_L, is defined as the difference in energy between the (symmetric) delocalized state and the (infinitesimally distorted) localized state; the Pauli repulsion energy, E_P, as the energy of the infinitesimally distorted hs-FM and AF_{II} states relative to ls-FM; and the relaxation energy, E_R, as the difference in energy between the infinitesimally distorted and minimum-energy distorted states.

As reported previously for Li:NiO [8] and NiO [9], further *direct* evidence for the essentially O(p) character of the self-trapped hole in MnO is contained in the charge- and net spin-density distributions of both the neutral and ionized states which are computed directly from the corresponding wavefunctions. Figure 3(a) shows the net spin density in a basal {001} plane of neutral (FM) Mn_8O_8 containing Mn_3, Mn_4, ..., O_1, O_2, ..., with O_1 the central atom. In agreement with the Mulliken populations given in table 1, there is near complete localization of the spin at the four Mn atoms and only very minor density at the five O atoms. Figures 3(b), 3(c) and 3(d) show the same net spin distributions for symmetry-broken (ls-FM) $Mn_8O_8^{(+)}$, (hs-FM) $Mn_8O_8^{(+)}$ and (AF_{II}) $Mn_8O_8^{(+)}$, corresponding to infinitesimally small (0.001 Å) displacements of Mn_5. It is evident that the spin density at the four Mn atoms and four outer O atoms is practically unchanged, whereas O_1 has acquired spin with a characteristic p_σ profile leading to a *highly localized* hole state in all three spin configurations. These figures also show that in the FM lattice there is a small,

but significant, dispersion of the spin at the oxygen sites in both the neutral and hole states, whereas there is no spin dispersion at the oxygen sites in the AF_{II} lattice by symmetry. This is all in complete agreement with the Mulliken population analyses.

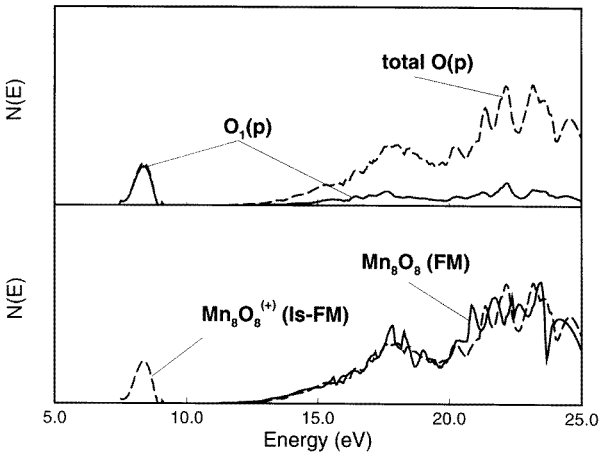

Figure 4. Upper panel: comparison of the total empty O(p) (dashed line) and O_1 projected empty p states (full line) of (ls-FM) $Mn_8O_8^{(+)}$; lower panel: comparison of the total empty O(p) states of (FM) Mn_8O_8 (dashed line) and (ls-FM) $Mn_8O_8^{(+)}$ (full line).

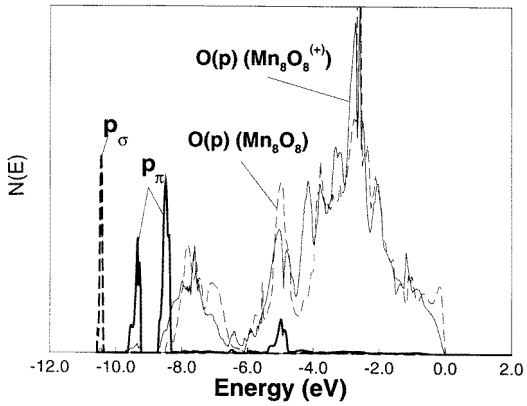

Figure 5. Comparison of the valence band (filled) O(p) DOS of (FM) Mn_8O_8 (light dashed line) and (ls-FM) $Mn_8O_8^{(+)}$ (p_σ orbital: heavy dashed line; p_π orbital: heavy full line; O(p): light full line).

Further confirmation as to the nature of the hole state in MnO is contained in the single-particle densities of states, and in particular comes from a comparison of the *empty* O(p) DOS of the neutral and hole states. Figure 4 shows this comparison for the (symmetry-broken) ls-FM state. It is evident that the removal of an electron leads to new empty O(p) states ∼3–4 eV below the conduction band edge (CBE), while leaving the conduction band states more or less unchanged, exactly as in NiO [9], and that these new states are localized almost entirely at O_1. For the hs-FM and AF_{II} configurations the overall DOS are very

similar, but with minor shifts of ∼0.1–0.2 eV in the position of the new empty O(p) states. As in the case of Li:NiO [8] and NiO [9] we note that the gap between the new empty O(p) states and the CBE is close to the measured gap of 3.8–4.2 eV in MnO [24]. The localized nature of the self-trapped hole is also evident from the valence band DOS. As figure 5 shows, while the DOS of the singly occupied p_σ and two doubly occupied p_π orbitals at O_1, the hole site, are shifted to lower energy as a result of the reduced on-site Coulomb repulsion, the DOS of the other O(p) electrons of the unit cell are largely unaffected by the presence of the hole and remain close to those of the neutral system.

Thus the picture of the *ground state* of the hole in MnO to emerge from these calculations is one in which the hole density is confined essentially to a *single* oxygen p_σ orbital with respect to the lattice distortion, with comparatively little perturbation of either the on-site electrons or those of the neighbouring ions.

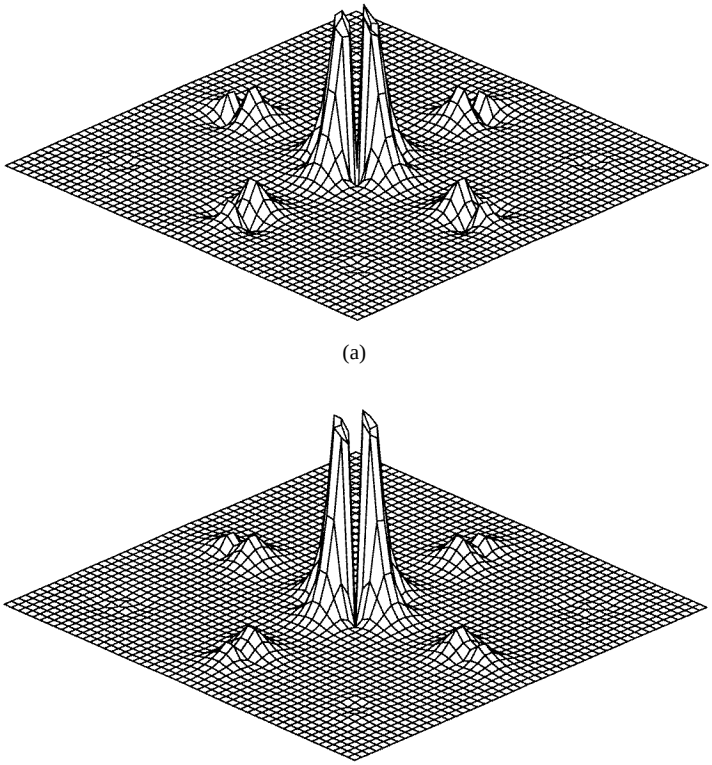

(a)

(b)

Figure 6. The difference in charge-density (a) and spin-density (b) distributions in a basal {100} plane between (AF_{II}) Mn_8O_8 and (AF^*_{II}) $Mn_8O_8^{(+)}$.

The calculations reported above illustrate an extremely useful, though not fully understood [25], aspect of UHF theory, namely the effect of symmetry breaking. For the hole state in MnO (and NiO), fully symmetric lattices lead to delocalized states, whereas symmetry-broken lattices, even in the limit of infinitesimal distortions, lead to electron configurations in which the hole/unpaired electron is strongly localized in a p_σ orbital at a *single* O site. We have found that the second of the two possible {100} distortions of AF_{II} $Mn_8O_8^{(+)}$, namely that in which the Mn of *opposite* spin to the unpaired electron is

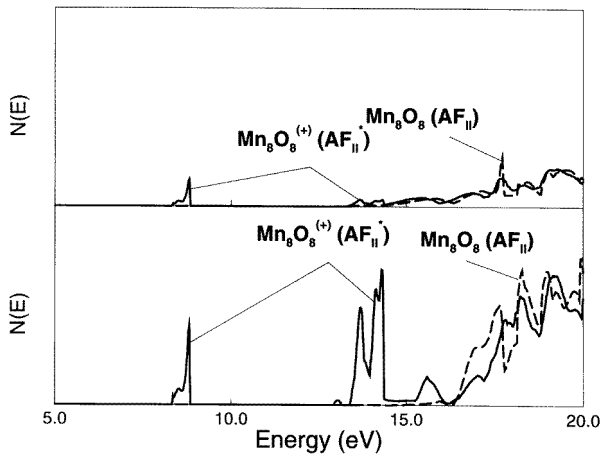

Figure 7. Comparison of the empty O(p) (upper panel) and Mn(d) (lower panel) DOS of (AF_{II}) Mn_8O_8 and (AF_{II}^*) $Mn_8O_8^{(+)}$.

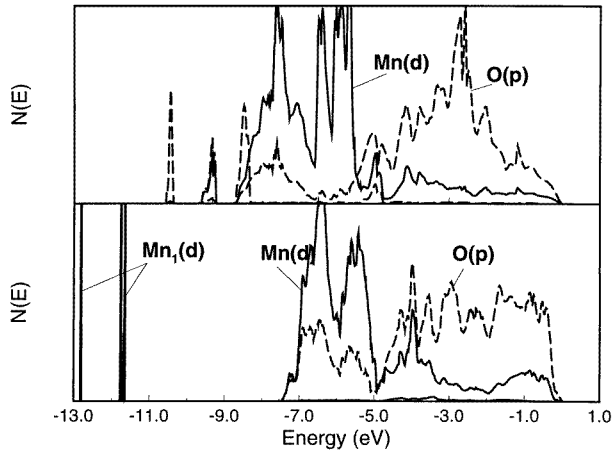

Figure 8. Comparison of the valence band DOS of (AF_{II}) $Mn_8O_8^{(+)}$ (upper panel) and (AF_{II}^*) $Mn_8O_8^{(+)}$ (lower panel).

displaced, leads to a different hole state 0.70 eV *higher* than before, in which the hole is localized largely in a $d_{x^2-y^2}$ orbital of a *single* Mn atom giving an $\sim d^4\ ^5E_g$ state. As shown in table 2, where this excited state is indicated as AF_{II}^*, a Mulliken analysis suggests that $\sim$50% of the hole is localized in this way and $\sim$30% at four nearest-neighbour oxygen sites. Once again, direct evidence of the nature of this state is contained in the charge and net spin distributions and densities of empty states. Figures 6(a) and 6(b) show the *differences* in charge and spin distributions in a basal {100} plane between the neutral (Mn_8O_8) and excited hole (AF_{II}^* $Mn_8O_8^{(+)}$) states where the dispersion of the hole at the *five* sites and the $d_{x^2-y^2}/p_\sigma$ character of the hole suggested by the Mulliken analysis is quite evident. The more diffuse nature of the hole is also what might be expected of an excited state. This picture of the excited hole state is confirmed by the empty O(p) DOS in figure 7 which shows only a small addition of states $\sim$4 eV below the CBE corresponding to the

localization of ∼30% of the hole at O sites. A more significant change is seen in the density of empty Mn(d) states both below the CBE as a result of d_σ–p_σ hybridization and at the band edge. Once again, the difference density distributions and densities of empty states are in complete agreement with the Mulliken analysis. For completeness, figure 8 the shows the valence band DOS where it is compared with that of the ground state. In the excited state there is a decrease in width (of the main part of the band) of ∼1 eV, and, as in the ground state, a shift to lower energy of the local states at the (majority) hole site, Mn_1, which form very narrow atomic-like states ∼5 eV below the main band.

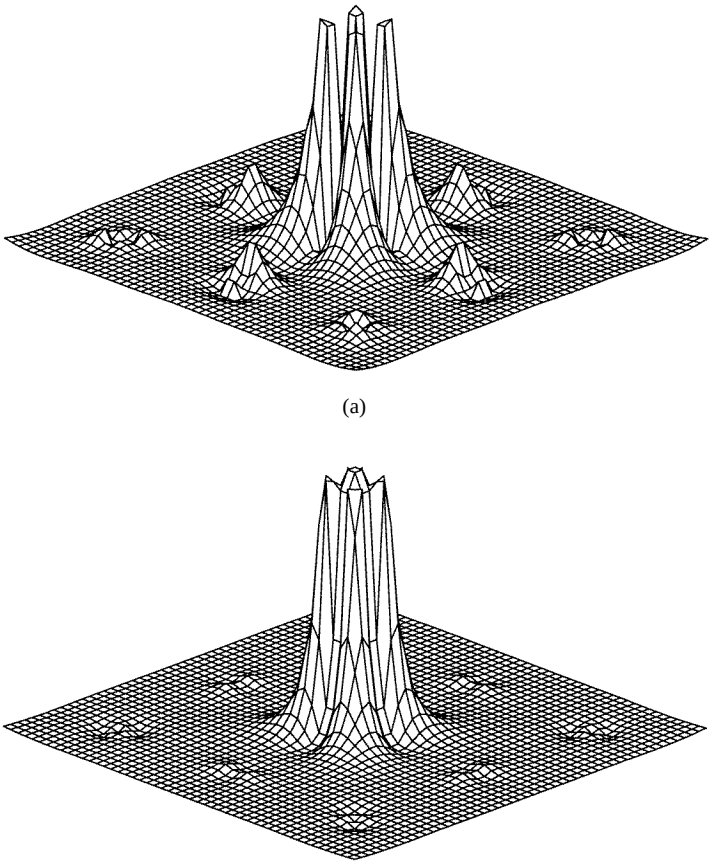

(a)

(b)

Figure 9. The difference in charge-density (a) and spin-density (b) distributions in a basal {100} plane between (FM) Mn_8O_8 and (FM) $Mn_8O_8^{(-)}$.

3.3. Electron addition states in MnO

There is much less controversy concerning the nature of the electron addition state in MnO which is generally accepted as d^6. This would follow from either a Mott–Hubbard or charge-transfer description of the oxide. What we are primarily interested in here is whether an added electron can self-trap or whether it requires a charged impurity such as a fluorine substitutional defect at an oxygen site. Our approach follows closely that for the hole state,

except that here we have confined our calculations to the FM state for which there is only one spin arrangement corresponding to the d^6 configuration. The addition of an electron to a fully symmetric FM lattice in which every site has O_h symmetry, leads to a state in which the added electron is delocalized over six Mn sites of the $Mn_8O_8^{(-)}$ super-cell no matter what starting electronic configuration is chosen. However, as in the case of the hole, the removal of this symmetry constraint allows the electronic configuration to relax to a non-degenerate state of lower energy, in which the added electron is localized on a *single* Mn site. In particular, a {100} displacement of O_3 (or any symmetry-equivalent atom) reduces the local symmetry of Mn_8 from O_h to C_{4v} which splits the degeneracy of the empty t_{2g} states at Mn_8. This leads to a localization of the added electron in a d_{xy} orbital giving a $^5T_{2g}$ state, with a relaxation energy of 0.07 eV at a displacement of 0.13 Å away from the trapped electron. However, unlike the case for the hole state, here we find the energy of the localized state to be 0.24 eV *higher* than that of the delocalized state. The *changes* in the Mulliken populations suggest that ∼76% of the added electron is localized at Mn_8. The corresponding calculations for Mn_8O_7F, on the other hand, find the localized $^5T_{2g}$ state, in which the added electron is again localized in a d_{xy} orbital, to be lower in energy than the delocalized state by 1.32 eV, with a relaxation energy of 0.07 eV for a displacement of 0.16 Å away from the trapped electron. Again a Mulliken population analysis suggests that ∼77% of the added electron is localized at a single Mn site. As in the case of hole states, *difference* charge- and spin-density distributions in a {100} basal plane between the neutral and ionized states provide direct confirmation of the Mulliken analysis. Thus figure 9 shows that the added charge density is localized largely at a single Mn site in a d_{xy} orbital, but with some dispersion at the nearest-neighbour O sites, whereas the *decrease* in the net spin density is confined exclusively to the Mn site.

4. Discussion

This paper has sought to clarify an important aspect of the electronic structure of MnO, namely the nature of its hole and electron addition states, in view its intermediate position in the ZSA phase diagram and a recent suggestion from UHF calculations that FeO is a Mott–Hubbard insulator [9]. As in the case of Li:NiO [8] and NiO [9], the aim here has been to investigate the nature of these states as *directly* as possible, by examining the charge- and net spin-density distributions in appropriate crystallographic planes and the atom-projected densities of single-particle states. These are used to confirm independent deductions of the nature of the defect state from Mulliken population analyses.

Mulliken population analyses of the UHF wavefunctions of periodic super-cells of Mn_8O_8 in both the FM and AF_{II} spin arrangements from which a single electron has been removed indicate that the resulting valence band hole is confined to the oxygen O(p) band in both the fully symmetric lattice structure and that containing a local distortion which reduces individual oxygen site symmetries from O_h to C_{4v} thereby splitting the degeneracy of the O(p) states. In the former, the unpaired electron/hole is delocalized over six symmetry-equivalent oxygen sites leading to a conducting state, whereas in the latter, the defect is localized in a p_σ orbital at a single oxygen site, as shown in figure 3(b). This leads to insulating states of lower energy, exactly as found previously for NiO [9], with localization energies in the range 2.33–2.51 eV for the three spin configurations that we have examined, which compare with a value of 3.3 eV for NiO [9]. Thus UHF calculations confirm MnO to be a high-spin $p \rightarrow d$ charge-transfer insulator with localized (small-polaron) free holes, in agreement with recent spectroscopic evidence given by Becker and He [26]. In addition, the relaxation energies of 0.14–0.20 eV, which correspond to the displacement of a nearest-

neighbour Mn atom away from the hole and hence to the energy of a {100} jump to a next-nearest-neighbour O site, are close to the reported activation energy of ∼0.3 eV for hole conductivity in Li-doped MnO [27] which is further support for a small-polaron model. The principal reason for localization is the increased polarization energy (of the localized state) which is proportional to the square of the effective charge, so the (electronic) polarization energy resulting from localization of a hole in fcc MnO is approximately six times that of a delocalized hole. This also accounts for the difference between MnO and NiO, for the polarizability of Ni(d^8) is greater than that of Mn(d^5), whereas the valence band widths of NiO and MnO, which determine the kinetic energy of the delocalized hole, are comparable. The localized state is further stabilized by the displacement dipole which results from the lattice relaxation *away* from the hole site as reported previously for Li:NiO [8] and NiO [9] and found experimentally for Li:MgO from ESR measurements [28].

Since the hole state in MnO formally represents Mn(III), this raises the question as to lattice distortions of the type which are often said, though seldom proved, to result from the Jahn–Teller (JT) mechanism associated with the Mn(d^4) configuration [1]. While our examination of lattice relaxation is by no means exhaustive, it has demonstrated quite clearly that a finite distortion *lowers* the energy of an unrelaxed (infinitesimally distorted) lattice with a localized O(p^5) hole in both the FM and AF_{II} arrangements. Thus UHF calculations suggest a reinterpretation of the distortion associated with Mn(III) in terms of displacement-dipole stabilization and/or a JT mechanism involving O(p^5) rather than Mn(d^4). This is precisely what was found previously for the hole state in NiO [8, 9] where distortions associated with Ni(III) are conventionally interpreted in terms of a JT mechanism involving Ni(d^7).

The differences in energy reported here between the three spin configurations reveal for the first time, we believe, the magnitude of the magnetic effects associated with the hole state, with $E(\text{ls-FM}) < E(\text{AF}_{\text{II}}) < E(\text{hs-FM})$. A close examination of the spin-density distributions reveals a confinement of the unpaired electron at the hole site in the hs-FM and AF_{II} states relative to ls-FM due to Pauli repulsion, with a noticeable asymmetry of the exclusion in AF_{II} as a direct consequence of the asymmetric spin arrangement in the lattice. The differences in energy of 0.71 eV and 0.29 eV for E_P(hs-FM) and $E_P(\text{AF}_{\text{II}})$ respectively, which we have referred to in table 4 as the Pauli (repulsion) energy, indicate that the increase in kinetic energy of the hs-FM and AF_{II} states (compared with ls-FM), which results from this confinement, is much greater than the direct spin–spin stabilization energy. Furthermore, our value of 0.29 eV (∼2500 K) for $E_P(\text{AF}_{\text{II}})$ is two orders of magnitude greater than the UHF super-exchange energy, 0.002 eV [7], which suggests that both above and below the Néel temperature (∼120 K) the free hole in MnO will have the characteristics of a spin polaron with a 'bag' of six *antiferromagnetic* nearest-neighbour d^5 spins. The differences in the magnetic energies are also greater than the lattice relaxation energy, 0.14–0.33 eV, which suggests that their neglect in atomistic simulations might be a source of significant error in such studies.

While it is clear from the results presented here that the UHF *ground* state of the hole in MnO is essentially $d^5\underline{L}$, the prediction of an excited state of ∼d^4 character 0.7 eV above the ground state is consistent with the intermediate position of MnO in the ZSA classification, even though the hole is not quite the almost equal mixture of O(p) and Mn(d) suggested by ZSA [2] and van Elp *et al* [3] who deduced weights of 0.50 and 0.42 for $d^5\underline{L}$ and d^4 respectively. In the terminology used by ZSA [2, 3] the difference in energy between $d^5\underline{L}$ and d^4 is approximately $\Delta - U$, where Δ is the charge-transfer energy and U the (on-site) d–d Coulomb energy. van Elp *et al* [3] reported a value of 0.3 eV for $\Delta - U$, which compares with our value of 0.7 eV for the AF_{II} lattice. Perhaps the most significant

consequence of the relatively small difference in energy between $d^5\underline{L}$ and d^4 reported here, and the even smaller difference suggested by van Elp *et al* [3], is that the valence states of Mn in Mn(III) and higher oxides are likely to vary from $\sim d^5$ to $\sim d^4$ depending on the composition, crystal structure and magnetic state of the oxide [29]. Reports of this in respect of Mn_3O_4 and $LiMnO_2$ are in preparation [30].

Our $^5T_{2g}$ d^6 description of the first electron addition state is consistent with that of van Elp *et al* [3] who found the $^5T_{2g}$ state to be $\sim$1 eV lower than ^5E_g with approximately equal contributions to the BIS spectrum [3]. The free state is predicted to be delocalized, which is to be expected in view of the width of the conduction band. This is consistent with measurements of the Hall mobility of n-type MnO, which at elevated temperatures is over three orders of magnitude greater than that of p-type MnO [27]. Substitutional F^- is predicted to localize the electron addition state with a total stabilization energy of $\sim$1.5 eV, which is consistent with a screened Coulombic interaction with an effective dielectric constant of $\sim$8.

5. Conclusions

The principal conclusions of this study are (i) that the ground state of the hole in MnO is essentially $d^5\underline{L}$ (^5E_g) in both the FM and AF_{II} spin arrangements and the electron addition state d^6, which confirms MnO as a p $\rightarrow$ d charge-transfer insulator; (ii) that the free hole is localized, leading to small-polaron behaviour, with localization and relaxation energies of $\sim$2.5 eV and 0.15 eV respectively; (iii) that the free hole is a spin polaron with fully antiferromagnetic d^5 nearest neighbours; (iv) that the origin of lattice distortion associated with Mn(III) can derive from a mechanism other than the d^4 Jahn–Teller one; (v) that the electron addition state is delocalized; (vi) that substitutional F^- localizes d^6 in a $^5T_{2g}$ state; (vii) that the description of hole and electron states in MnO derived from Mulliken population analyses are in complete agreement with those from charge- and spin-density distributions and atom-projected densities of valence band states, as previously noted for Li-doped NiO and NiO; and (viii) that the distribution of states at the VBE and CBE are a reliable guide to the nature of the hole and electron states.

Acknowledgments

WCM would like to thank Professor G A Sawatzky for an extremely informative discussion on aspects related to this paper. E-AW wishes to thank the University of St Andrews (Purdie Fund) for the award of a research studentship. The work was also supported by EPSRC grant GK/K06389.

References

[1] Cox P A 1990 *Transition Metal Oxides* (Oxford: Oxford University Press)
[2] Zaanen J, Sawatzky G A and Allen J W 1984 *Phys. Rev. Lett.* **55** 418
[3] van Elp J, Potze R H, Eskes H, Berger R and Sawatzky G A 1991 *Phys. Rev.* B **44** 1530
[4] Svane A and Gunnarsson O 1990 *Phys. Rev. Lett.* **65** 1148
[5] Terakura K, Oguchi T, Williams A R and Kuebler J 1984 *Phys. Rev.* B **30** 4734
[6] Mackrodt W C, Harrison N M, Saunders V R, Allan N L, Towler M D, Aprà E and Dovesi R 1993 *Phil. Mag.* A **68** 653
[7] Towler M D, Allan N L, Harrison N M, Saunders V R, Mackrodt W C and Aprà E 1994 *Phys. Rev.* B **50** 5041
[8] Mackrodt W C, Harrison N M, Saunders V R, Allan N L and Towler M D 1996 *Chem. Phys. Lett.* **250** 66

[9] Mackrodt W C 1997 *Ber. Bunsenges. Phys. Chem.* **101** 169
[10] Kuiper P, Kruizinga G, Ghijsen J and Sawatzky G A 1989 *Phys. Rev. Lett.* **62** 221
[11] van Elp J, Searle B G, Sawatzky G A and Sacchi M 1991 *Solid State Commun.* **80** 67
[12] van Elp J, Eskes H, Kuiper P and Sawatzky G A 1992 *Phys. Rev.* B **45** 1612
[13] Springhorn C and Schmalzried H 1994 *Ber. Bunsenges. Phys. Chem.* **98** 746
[14] Towler M D, Allan N L, Harrison N M, Saunders V R and Mackrodt W C 1995 *J. Phys.: Condens. Matter* **7** 6231
[15] Mott N F 1974 *Metal–Insulator Transitions* (London: Barnes and Noble)
[16] Alexandrov A S and Mott N F 1994 *High T_c Superconductors and other Superfluids* (London: Taylor and Francis)
[17] Anisimov V I, Korotin M A, Zaanen J and Andersen O K 1992 *Phys. Rev. Lett.* **68** 345
[18] Dovesi R, Saunders V R, Roetti C, Causà M, Harrison N M, Orlando R and Aprà E 1995 *CRYSTAL 95 User Manual* Università di Torino and CCLRC Daresbury Laboratory
[19] Pisani C, Dovesi R and Roetti C 1988 *Hartree–Fock Ab Initio Treatment of Crystalline Systems* (Berlin: Springer)
[20] Pople J A and Nesbet R K 1954 *J. Chem. Phys.* **22** 571
[21] Dovesi R, Causà M, Orlando R, Roetti C and Saunders V R 1990 *J. Chem. Phys.* **92** 7402
[22] Monkhorst H J and Pack J D 1976 *Phys. Rev.* B **13** 5188
[23] Mulliken R S 1955 *J. Chem. Phys.* **23** 1833
Mulliken R S 1955 *J. Chem. Phys.* **23** 1841
[24] Drabkin I A, Emel'yanova L T, Iskenderov R N and Ksendzov Y M 1968 *Fiz. Tverd. Tela* **10** 3082 (Engl. Transl. 1969 *Sov. Phys.–Solid State* **10** 2428)
[25] Fukutome H 1981 *Int. J. Quantum Chem.* **20** 955
[26] Becker K D and He T 1992 *Ber. Bunsenges. Phys. Chem.* **96** 1886
[27] Crevecoeur C and de Wit H J 1970 *J. Phys. Chem. Solids* **31** 783
[28] Abraham M M, Chen Y and Unruh W P 1974 *Phys. Rev.* B **9** 1842
[29] Mackrodt W C and Simson E-A 1996 *J. Chem. Soc. Faraday Trans.* II **92** 2043
[30] Mackrodt W C and Williamson E-A 1997 *Ber. Bunsenges. Phys. Chem.* at press